

NASA/TM—2006-214088



Life Limiting Behavior in Interlaminar Shear of Continuous Fiber-Reinforced Ceramic Matrix Composites at Elevated Temperatures

Sung R. Choi
University of Toledo, Toledo, Ohio

Anthony M. Calomino, Narottam P. Bansal, and Michael J. Verrilli
Glenn Research Center, Cleveland, Ohio

January 2006

The NASA STI Program Office . . . in Profile

Since its founding, NASA has been dedicated to the advancement of aeronautics and space science. The NASA Scientific and Technical Information (STI) Program Office plays a key part in helping NASA maintain this important role.

The NASA STI Program Office is operated by Langley Research Center, the Lead Center for NASA's scientific and technical information. The NASA STI Program Office provides access to the NASA STI Database, the largest collection of aeronautical and space science STI in the world. The Program Office is also NASA's institutional mechanism for disseminating the results of its research and development activities. These results are published by NASA in the NASA STI Report Series, which includes the following report types:

- **TECHNICAL PUBLICATION.** Reports of completed research or a major significant phase of research that present the results of NASA programs and include extensive data or theoretical analysis. Includes compilations of significant scientific and technical data and information deemed to be of continuing reference value. NASA's counterpart of peer-reviewed formal professional papers but has less stringent limitations on manuscript length and extent of graphic presentations.
- **TECHNICAL MEMORANDUM.** Scientific and technical findings that are preliminary or of specialized interest, e.g., quick release reports, working papers, and bibliographies that contain minimal annotation. Does not contain extensive analysis.
- **CONTRACTOR REPORT.** Scientific and technical findings by NASA-sponsored contractors and grantees.

- **CONFERENCE PUBLICATION.** Collected papers from scientific and technical conferences, symposia, seminars, or other meetings sponsored or cosponsored by NASA.
- **SPECIAL PUBLICATION.** Scientific, technical, or historical information from NASA programs, projects, and missions, often concerned with subjects having substantial public interest.
- **TECHNICAL TRANSLATION.** English-language translations of foreign scientific and technical material pertinent to NASA's mission.

Specialized services that complement the STI Program Office's diverse offerings include creating custom thesauri, building customized databases, organizing and publishing research results . . . even providing videos.

For more information about the NASA STI Program Office, see the following:

- Access the NASA STI Program Home Page at <http://www.sti.nasa.gov>
- E-mail your question via the Internet to help@sti.nasa.gov
- Fax your question to the NASA Access Help Desk at 301-621-0134
- Telephone the NASA Access Help Desk at 301-621-0390
- Write to:
NASA Access Help Desk
NASA Center for Aerospace Information
7121 Standard Drive
Hanover, MD 21076



Life Limiting Behavior in Interlaminar Shear of Continuous Fiber-Reinforced Ceramic Matrix Composites at Elevated Temperatures

Sung R. Choi
University of Toledo, Toledo, Ohio

Anthony M. Calomino, Narottam P. Bansal, and Michael J. Verrilli
Glenn Research Center, Cleveland, Ohio

National Aeronautics and
Space Administration

Glenn Research Center

Acknowledgments

This work was supported by the Ultra-Efficient Engine Technology (UEET) Project, NASA Glenn Research Center, Cleveland, Ohio. The authors are grateful to R. Pawlik for experimental work during the course of this work.

This report is a formal draft or working paper, intended to solicit comments and ideas from a technical peer group.

Trade names or manufacturers' names are used in this report for identification only. This usage does not constitute an official endorsement, either expressed or implied, by the National Aeronautics and Space Administration.

Available from

NASA Center for Aerospace Information
7121 Standard Drive
Hanover, MD 21076

National Technical Information Service
5285 Port Royal Road
Springfield, VA 22100

Available electronically at <http://gltrs.grc.nasa.gov>

Life Limiting Behavior in Interlaminar Shear of Continuous Fiber-Reinforced Ceramic Matrix Composites at Elevated Temperatures

Sung R. Choi
University of Toledo
Toledo, Ohio 43606

Anthony M. Calomino, Narottam P. Bansal, and Michael J. Verrilli
National Aeronautics and Space Administration
Glenn Research Center
Cleveland, Ohio 44135

Abstract

Interlaminar shear strength of four different fiber-reinforced ceramic matrix composites was determined with double-notch shear test specimens as a function of test rate at elevated temperatures ranging from 1100 to 1316 °C in air. Life limiting behavior, represented as interlaminar shear strength degradation with decreasing test rate, was significant for 2-D crossplied SiC/MAS-5 and 2-D plain-woven C/SiC composites, but insignificant for 2-D plain-woven SiC/SiC and 2-D woven Sylramic SiC/SiC composites. A phenomenological, power-law delayed failure model was proposed to account for and to quantify the rate dependency of interlaminar shear strength of the composites. Additional stress rupture testing in interlaminar shear was conducted at elevated temperatures to validate the proposed model. The model was in good agreement with SiC/MAS-5 and C/SiC composites, but in poor to reasonable agreement with Sylramic SiC/SiC. Constant shear stress-rate testing was proposed as a possible means of life prediction testing methodology for ceramic matrix composites subjected to interlaminar shear at elevated temperatures when short lifetimes are expected.

1. Introduction

Successful development and design of continuous fiber-reinforced ceramic matrix composites (CMCs) are dependent on understanding their properties such as deformation, fracture, delayed failure (fatigue, slow crack growth, or damage accumulation), and environmental durability. Particularly, accurate evaluation of delayed failure behavior under specified loading/environment conditions is prerequisite to ensure accurate life prediction of structural CMC components at elevated temperatures.

Although fiber-reinforced CMCs have shown improved resistance to fracture and increased damage tolerance compared with monolithic ceramics, inherent material/processing defects or cracks in the matrix-rich interlaminar regions can still cause delamination under interlaminar normal or shear stress, resulting in loss of stiffness or in some cases structural failure. Strength behavior of CMCs in shear has been characterized in view of their unique interfacial architectures and its importance in structural applications (refs. 1 to 4). Because of the inherent nature of CMCs, it would be highly feasible that interlaminar defects or cracks are susceptible to delayed failure particularly at elevated temperatures, resulting in strength degradation or shortened time to failure. Although delayed failure is one of the important life-limiting phenomena, few studies have been done on this subject for CMCs under *shear* at elevated temperatures.

In a previous study (ref. 5), both interlaminar and in-plane shear strengths of a unidirectional Hi-Nicalon™ SiC fiber-reinforced barium strontium aluminosilicate (SiC/BSAS) composite were determined at 1100 °C in air as a function of test rate using double-notch shear test specimens. The composite exhibited a significant effect of test rate on shear strength, regardless of orientation. The shear strength degraded by about 50 percent as test rate decreased from the highest (10² MPa/s) to the lowest

(10^{-2} MPa/s). A phenomenological, life-prediction model has been proposed and formulated to account for the shear strength degradation of the composite.

This paper, as an extension of the previous study, describes life limiting behavior in interlaminar shear of four different fiber-reinforced CMCs at elevated temperatures, including three SiC fiber-reinforced CMCs and one carbon-fiber reinforced CMC. Interlaminar shear strength of each composite was determined in double notch shear as a function of test rate using constant stress-rate testing. The interlaminar shear strength was analyzed using the power-law type of crack growth model proposed previously in order to quantify the rate dependency/delayed failure of the composites under interlaminar shear. Stress rupture testing in interlaminar shear was also conducted at elevated temperatures with three selected CMCs in order to validate the proposed model. Some of the data in this paper have been reported previously (ref. 6).

2. Experimental Procedures

Four different CMCs—three SiC fiber-reinforced and one carbon fiber-reinforced—were used in this study, including Nicalon™ SiC 2-D crossplied fiber-reinforced magnesium aluminosilicate (designated SiC/MAS-5), Nicalon™ SiC 2-D plain-woven silicon carbide (designated SiC/SiC), Sylramic SiC 2-D woven silicon carbide (designated Sylramic SiC/SiC), and T300™ carbon-fiber 2-D plain-woven silicon carbide (designated C/SiC).

The SiC/MAS-5 composites were fabricated through hot pressing followed by ceramizing of the composites by a thermal process. The matrix was doped with 5 vol% of borosilicate glass to increase oxidation resistance and interfacial shear strength at the fiber/matrix interfaces. The silicon carbide matrix in the SiC/SiC composite was processed through chemical vapor infiltration (CVI) into the fiber preforms. Silicon carbide was also chemically vapor deposited onto the composite panels to cover the residual porosity. More detailed information regarding the processing of these SiC/MAS-5 and SiC/SiC composites can be found elsewhere (ref. 7). The Sylramic cloth preforms in the Sylramic SiC/SiC composite were stacked and chemically vapor infiltrated with a thin BN-based interface coating followed by SiC matrix over-coating. Remaining matrix porosity was filled with SiC particulates and then with molten silicon at 1400 °C, a process termed slurry casting and melt infiltration (ref. 8). Mechanical properties and fabrication and testing of vane subelements using the Sylramic SiC/SiC composites have been evaluated and addressed extensively in recent studies (refs. 9 to 11). The carbon fiber performs in the C/SiC composite were coated with pyrolytic carbon as an interface prior to CVI SiC infiltration (ref. 12). Stress/life behavior of the C/SiC composites has been characterized in a low partial pressure of oxygen at elevated temperatures (refs. 12 and 13). Fiber volume fraction, laminate architecture, nominal dimensions of shear test specimens, and other information of the CMCs used in this work are summarized in table 1. Weaving patterns of the CMCs are also shown in figure 1.

The double-notch-shear (DNS) test specimens were machined from panels of each CMC. Typically, test specimens were 13 to 15 mm wide (W) and 30 mm long (L). The thickness of test specimens was the same as a nominal thickness of panels of each composite (see table 1). Two notches, 0.3 mm wide (h) and 6 mm (Ln) away from each other, were made into each test specimen such that the two notches were extended to the middle of each specimen within ± 0.05 mm so that shear failure occurred on the plane between the notch tips. Schematics of DNS test specimen showing a notch configuration is shown in figure 2. Monotonic shear testing for DNS test specimens was conducted at elevated temperatures with different test rates in ambient air (relative humidity of about 45 percent), using an electromechanical test frame (Model 8562, Instron, Canton, Massachusetts) under load control. This type of testing, employing with different test rates, is called constant stress-rate or “dynamic fatigue” testing that is used for advanced monolithic ceramics and other brittle materials such as glasses and glass ceramics in order to evaluate their slow crack growth behavior in flexure or in tension (refs. 14 and 15). Test temperatures were 1100, 1200, 1316, and 1200 °C, respectively, for SiC/MAS-5, SiC/SiC, Sylramic SiC/SiC, and C/SiC composites.

TABLE 1.—FIBER-REINFORCED CERAMIC MATRIX COMPOSITES USED IN THIS WORK

Composites	Weaving	Fiber	Fiber volume fraction	Panels/notches	Manufacturer
SiC/MAS-5 ('93)	2-D cross-ply (0/90°)	Nicalon [#] SiC	0.39	16 plies; $t = 3.2$ mm; $W = 12.7$ mm; $L_n = 6$ mm	Corning, Inc. (Corning, NY)
SiC/SiC ('92)	2-D plain woven	Nicalon SiC	0.39	6.7 epc [§] ; 12 plies; $t = 3.5$ mm; $W = 13.0$; $L_n = 6$ mm	DuPont Lanxide Composites (now GE Power Systems Composites, GE PSC) (Newark, DE)
Sylramic SiC/SiC ('99)	2-D woven	Sylramic* SiC	0.36	7.9 epc; 5 HS; 8 plies; $t = 2$ mm; $W = 12.7/6$ mm; $L_n = 6$ mm	Honeywell Advanced Composites, Inc. (now GE PSC) (Newark, DE)
C/SiC ('97)	2-D plain woven	T300 [§] carbon	0.46	7.5 epc; 26 plies; $t = 3.3$ mm; $W = 15.4$ mm; $L_n = 6$ mm	Honeywell Advanced Composites, Inc. (now GE PSC) (Newark, DE)

[#] Nippon Carbon Co. (Japan)

*Dow Corning (Midland, MI)

[§] Toray Industries, Inc. (Japan)

[§] epc = end per centimeter.

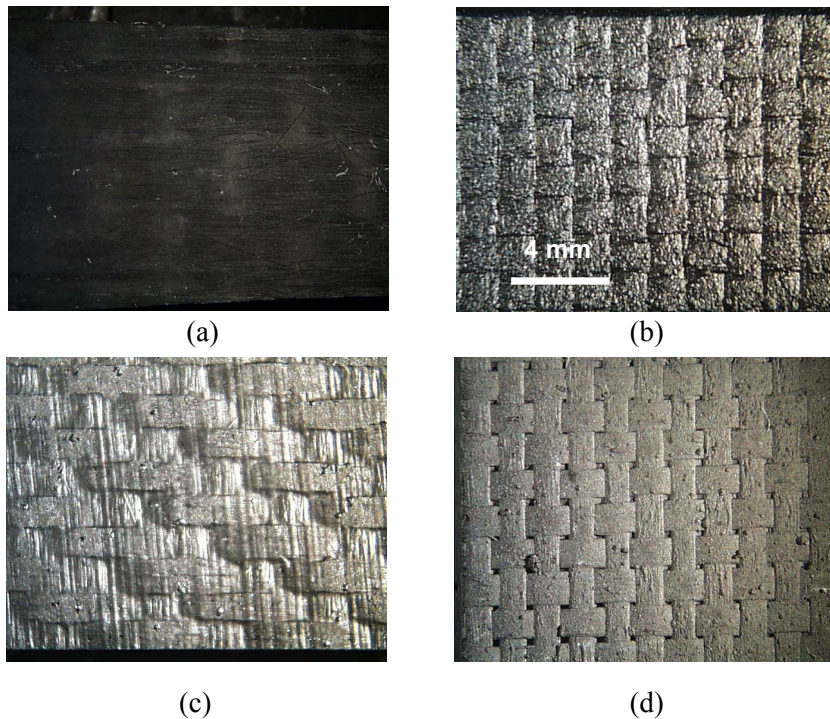


Figure 1.—Weaving patterns of continuous fiber-reinforced ceramic matrix composites used in this work: (a) SiC/MAS-5 (2-D cross-ply); (b) SiC/SiC (2-D plain-woven); (c) Sylramic SiC/SiC (2-D woven); (4) C/SiC (2-D plain-woven).

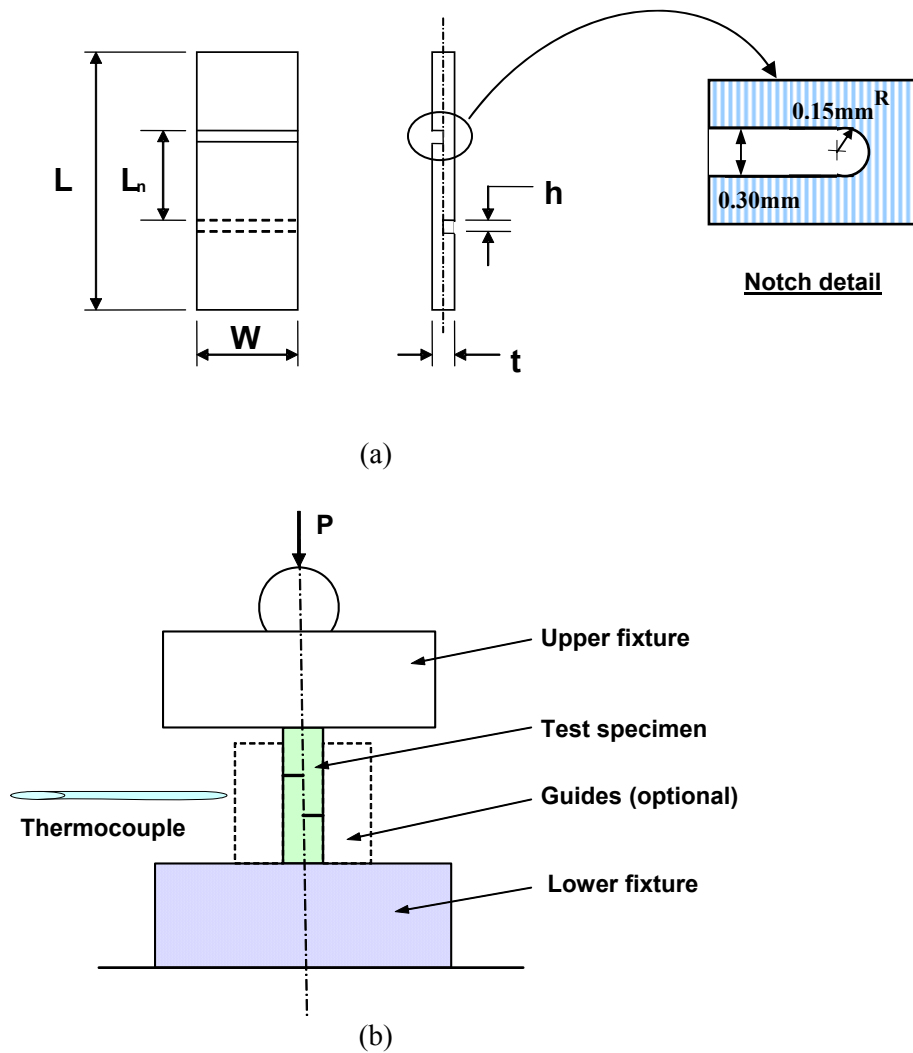


Figure 2.—(a) Configurations of double notch shear (DNS) test specimen; (b) A schematic showing test fixture and test specimen used in this work.

A total of three to four applied interlaminar shear stress rates ranging from 10^{-4} to 10^1 MPa/s were used for a given composite, depending on the type of composite. Typically, three to ten test specimens were tested at each test rate, again depending on type and availability of materials. A simple test-fixture configuration consisting of SiC upper and lower fixtures, as shown in figure 2, was used for test specimens whose thickness was ≥ 3 mm. With this specimen thickness and the tight machining tolerances, the test specimens could stand alone and be subjected to negligible bending (≤ 4 percent) due to misalignment, geometrical inaccuracies, and/or buckling. By contrast, for thin test specimens whose thickness was about 2 mm (e.g., Sylramic SiC/SiC composite), anti-buckling guides were used with specially designed ring-shaped fixtures. Each test specimen was kept for about 20 min at test temperature for thermal equilibration prior to testing. Basically, test specimen configurations and testing procedures were followed in accordance with ASTM test method C 1425 (ref. 16). The interlaminar shear fracture stress—the average interlaminar shear stress at failure—was calculated using the following relation

$$\tau_f = \frac{P_f}{WL_n} \quad (1)$$

where τ_f is the interlaminar shear strength, P_f is the fracture force, and W and L_n are the specimen width and the distance between the two notches, respectively (see fig. 2). The applied interlaminar shear stress rate $\dot{\tau}$ was given as follows:

$$\dot{\tau} = \frac{\dot{P}}{WL_n} \quad (2)$$

where \dot{P} is applied shear (or compressive) force rate employed via a test frame in load control.

Additionally, stress rupture testing in interlaminar shear was conducted with DNS test specimens for SiC/MAS-5 at 1100 °C, Sylramic SiC/SiC at 1316 °C, and C/SiC at 1200 °C in air. The test frame, test specimen configuration, and test fixture used in stress rupture were the same as those used in constant stress-rate testing. For each composite, the number of applied shear stresses was typically three, and the minimum number of test specimens used was six. This stress rupture testing was performed to determine life limiting behavior of the chosen composites under constant applied shear stress and to relate their stress rupture data to the respective constant stress-rate data in order to validate the phenomenological life prediction model proposed.

3. Experimental Results

3.1. Constant Stress-Rate Testing

Without exception, all specimens tested failed in interlaminar shear mode along their prospective shear planes. A typical example of a tested specimen showing such interlaminar shear mode failure is presented in figure 3, together with a test specimen prior to testing for comparison.

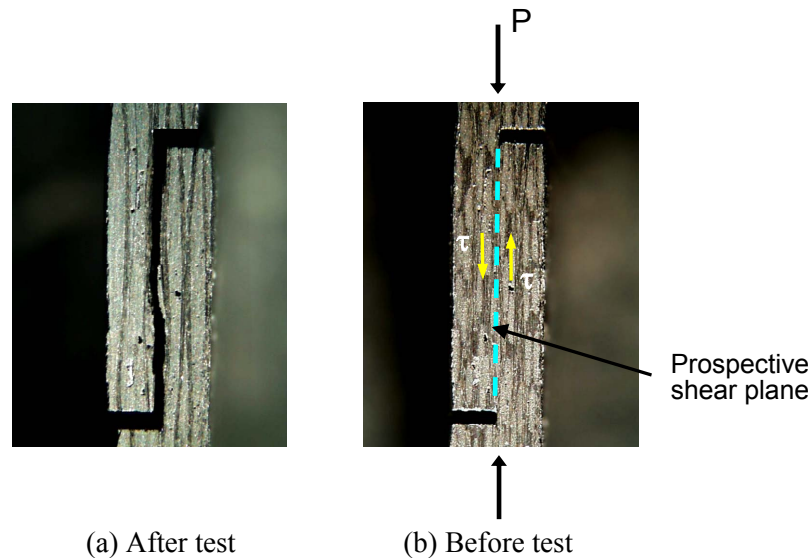


Figure 3.—(a) A typical example showing interlaminar shear failure of a Sylramic SiC/SiC composite double-notch-shear (DNS) specimen tested at 1316 °C in air at 5 MPa/s. The corresponding specimen configuration prior to test is shown in (b) for comparison. Note a slight change of specimen surface appearance due to high temperature exposure/oxidation.

3.1.1. SiC/MAS-5 Composite

The results of monotonic interlaminar shear strength testing for the 2-D crossplied SiC/MAS-5 composite tested at 1100 °C are presented in figure 4, where *interlaminar shear strength* is plotted as a function of *applied shear test rate*. The solid line in the figure represents a best-fit regression based on the log (*interlaminar shear strength*) versus log (*applied shear test rate*) relation. The reason for using the log-log relation will be described in the “Discussion” section. The decrease in interlaminar shear strength with decreasing test rate, indicating a susceptibility to delayed failure or slow crack growth, was significant for this composite. The interlaminar shear strength degradation was about 50 percent when test rate decreased from the highest (5 MPa/s) to the lowest (0.005 MPa/s) value. A similar trend in shear strength degradation with decreasing test rate was also found from a previous study in an 1-D, Hi-Nicalon™ fiber-reinforced barium strontium aluminosilicate (SiC/BSAS) composite at 1100 °C in air (ref. 5). This trend in shear strength with respect to test rate was also analogous to that in ultimate tensile strength of various continuous fiber-reinforced CMCs including SiC/MAS-5, SiC/CAS (calcium aluminosilicate), SiC/BSAS, C/SiC, and SiC/SiC composites (refs. 17 and 18). These CMCs have exhibited significant degradation of ultimate tensile strength with decreasing test rates, with their degree of degradation being dependent on material and test temperature.

Fracture surfaces of the SiC/MAS-5 composite showed that the mode of interlaminar shear failure was typified as delamination of fibers from matrix-rich regions, implying that the fiber-matrix interfacial architecture is the most influencing characteristic in controlling shear properties of the composite. More violent and rough fracture surfaces were seen from the specimens at higher test rate, sometimes exposing two more layers (0/90°) therein, while smoother surfaces were noted for the specimens at lower test rate with only one layer associated with delamination, as shown in figure 5. The presence of viscous flow/phases was obvious from fracture surfaces, particularly at low test rates in which more enhanced delayed failure occurred. The residual glassy phase might have been a major cause of delayed failure in the SiC/MAS-5 *silicate* composite, as observed previously in the SiC/BSAS *silicate* composite (ref. 5).

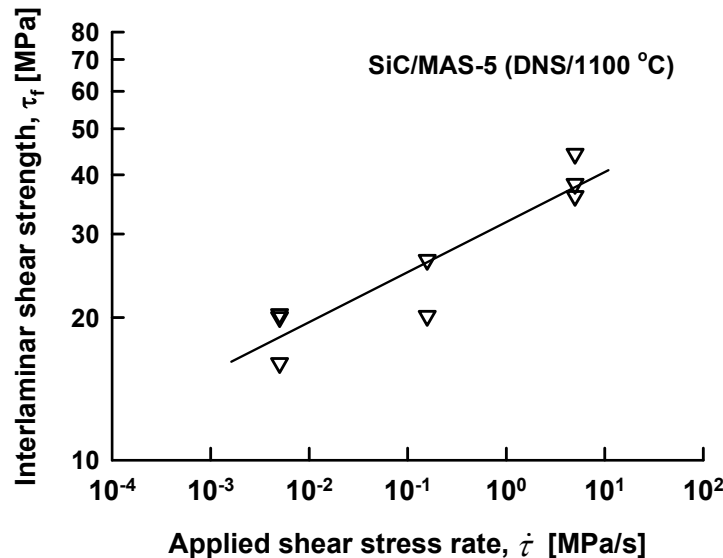


Figure 4.—Results of interlaminar shear strength as a function of applied shear stress rate for 2-D crossplied SiC/MAS-5 composite tested at 1100 °C in air. The solid line represents the best-fit.

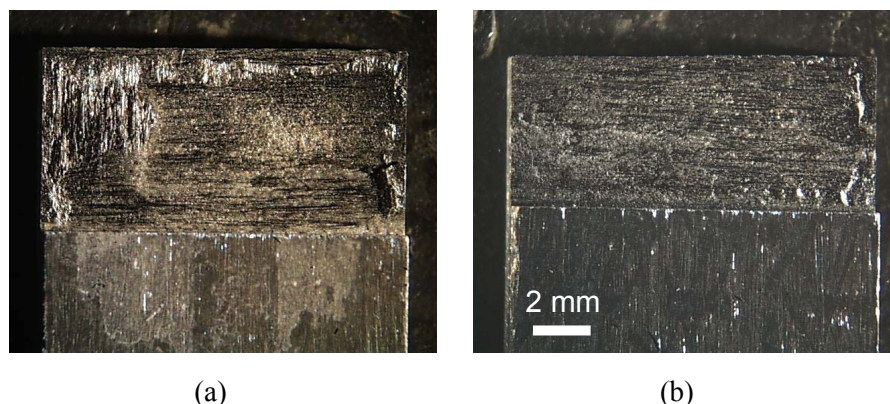


Figure 5.—Fracture surfaces of 2-D crossplied SiC/MAS-5 composite specimens subjected to interlaminar shear, tested at 1100 °C in air at: (a) 5 MPa/s and (b) 0.005 MPa/s.

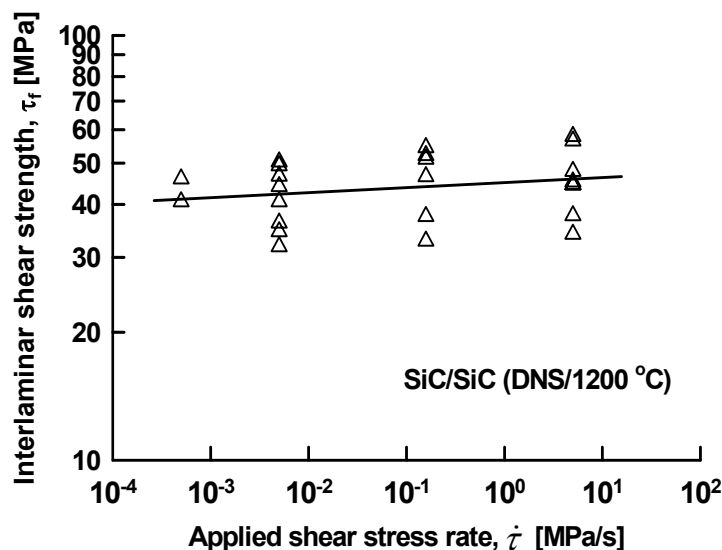


Figure 6.—Results of interlaminar shear strength as a function of applied shear stress rate for 2-D plain-woven SiC/SiC composite tested at 1200 °C in air. The solid line represents the best-fit.

3.1.2. SiC/SiC Composite

Figure 6 shows the results for the 2-D plain-woven SiC/SiC composite tested at 1200 °C, in which interlaminar shear strength was plotted in the same way as in figure 4, with the line representing the best-fit. Unlike the SiC/MAS-5 composite, the SiC/SiC composite did not exhibit any significant interlaminar strength degradation with decreasing test rate. The strength degradation from the highest (= 5 MPa/s) to the lowest (0.0005 MPa/s) test rate was only 5 percent, indicating a greater resistance to delayed failure or slow crack growth, compared with the SiC/MAS-5 composite. The corresponding two-parameter Weibull interlaminar shear strength distribution with the all the data in figure 6 combined is depicted in figure 7.

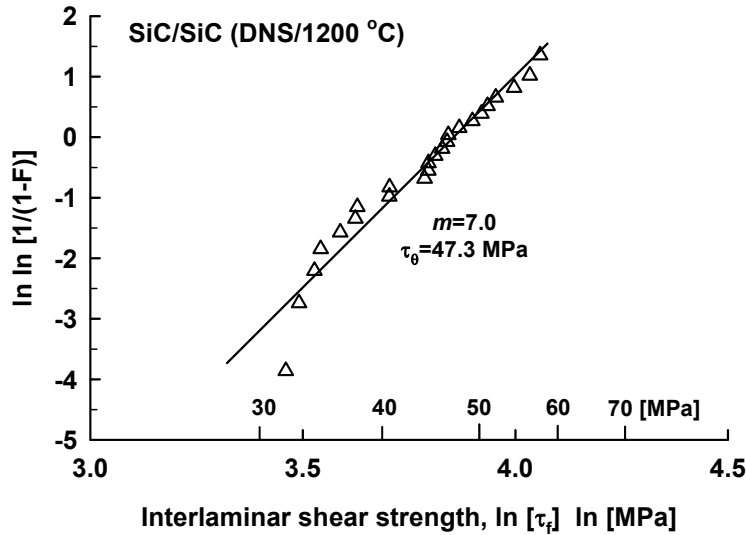


Figure 7.—Two-parameter Weibull interlaminar shear strength distribution of 2-D plain-woven SiC/SiC composite tested at 1200 °C in air, with all the data combined in figure 6. m : Weibull modulus; τ_0 : characteristic interlaminar shear strength; F : failure probability.



Figure 8.—Fracture surfaces of 2-D plain-woven SiC/SiC composite specimens subjected to interlaminar shear, tested at 1316 °C in air at: (a) 5 MPa/s and (b) 0.005 MPa/s.

Weibull modulus of interlaminar shear strength was $m = 7$, somewhat lower than the typical range of 10 to 20 for flexure or tensile strength of many monolithic ceramics. The characteristic (τ_0) and mean shear strengths were 47.3 and 44.3 ± 7.5 MPa, respectively. Fracture surfaces showed that some oxidation occurred therein with a bluish discoloration, (see fig. 8). Of course, more discoloration at lower test rates, and vice versa. Fracture surfaces also exhibited that well developed interlaminar shear occurred in matrix-rich regions between two adjacent laminates by delamination. Except for discoloration, the difference in fracture surface of test specimens between high and low test rates appeared to be unnoticeable.

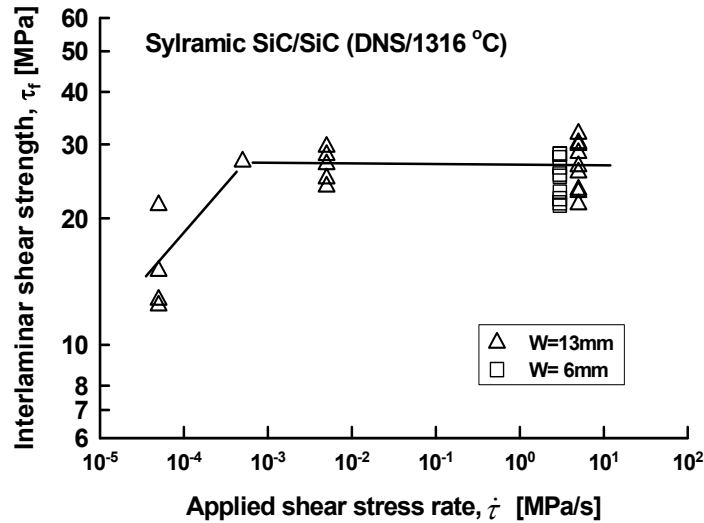


Figure 9.—Results of interlaminar shear strength as a function of applied shear stress rate for 2-D woven Sylramic SiC/SiC composite tested at 1316 °C in air. The data determined with test specimen's width of $W = 6$ mm are also included for comparison. The solid line represents the best-fit.

3.1.3. Sylramic SiC/SiC Composite

The results of interlaminar shear strength testing for the 2-D woven Sylramic SiC/SiC composite at 1316 °C are depicted in figure 9. The composite exhibited no apparent shear strength degradation down to 0.0005 MPa/s; however, it exhibited strength degradation at the lowest test rate of 0.00005 MPa/s, resulting in an about 40 percent reduction in average shear strength. The test time corresponding to the lowest test rate was around 85 hr so that this long duration of test would have caused such significant strength degradation through a possible environmental degradation. Invariably, a severe discoloration was observed from the surfaces of specimens tested at this test rate, as shown in figure 10. The pattern of shear fracture was such that an apparent shear delamination with little damage in fiber tows was evident from the fracture surfaces of specimens tested at lower test rates, while rough fracture surfaces with a somewhat plucking mode in fiber tows were typified at higher test rates, as seen from figure 10. In terms of duration of test time, a question arises as to whether strength degradation would take place if an extremely low test rate of 0.00005 MPa/s, which was applied for the Sylramic SiC/SiC composite, is employed to the 2-D plain-woven SiC/SiC composite. A further investigation is needed.

It is important to note that the size effect on interlaminar shear strength was negligible for the Sylramic SiC/SiC composite, as seen in figure 9, where interlaminar shear strength of additional test specimens with $W = 6$ mm, determined at the same test rate of 5 MPa/s, was compared with that of the regular test specimens with $W = 13$ mm. The average interlaminar shear strength of 10 test specimens was 27 ± 4 and 25 ± 3 MPa, respectively, for $W = 13$ and 6 mm. Also, considering that overall interlaminar shear strength was not changed significantly regardless of test rate > 0.00005 MPa/s, it could be possible to take all strength values at different test rates as single representing data. With this approach, two-parameter Weibull interlaminar strength distributions were obtained and the results are shown in figure 11. Weibull modulus ($m = 10.7$ vs. 10.4) as well as characteristic shear strength ($\tau_0 = 28$ vs. 26 MPa) is about the same for both specimen sizes. It is noted that the value of Weibull modulus for the Sylramic SiC/SiC, $m \approx 10$, compares reasonably well with $m = 7$ for the 2-D plain-woven SiC/SiC (see fig. 7).

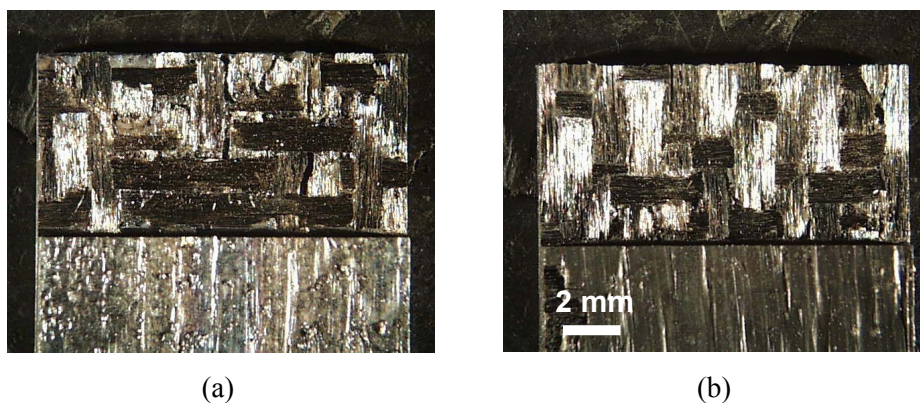


Figure 10.—Fracture surfaces of 2-D woven Sylramic SiC/SiC composite specimens subjected to interlaminar shear, tested at 1316 °C in air at: (a) 5 MPa/s and (b) 0.00005 MPa/s.

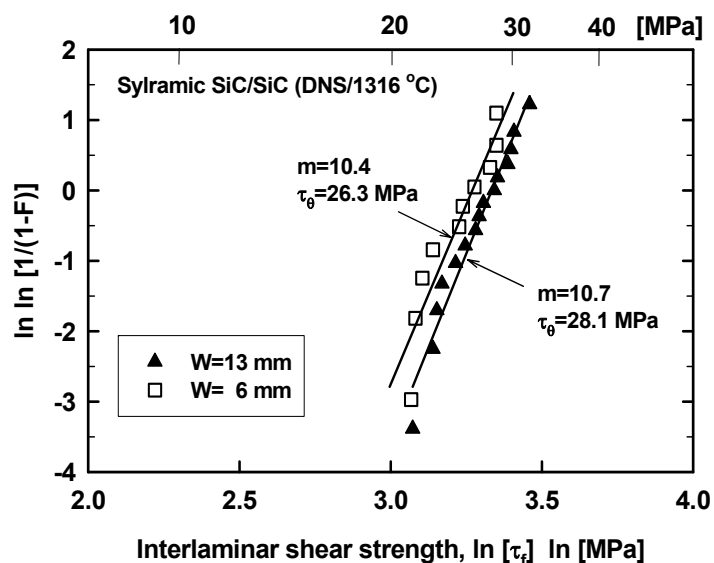


Figure 11.—Weibull interlaminar shear strength distributions of two different sizes ($W = 13$ and 6 mm) of double-notch shear test specimens of 2-D woven Sylramic SiC/SiC composite tested at 5 MPa/s at 1316 °C in air.

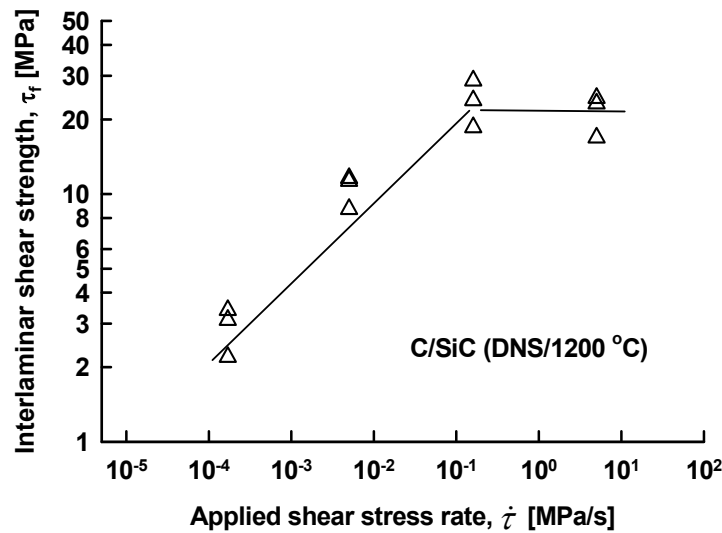


Figure 12.—Results of interlaminar shear strength as a function of applied shear stress rate for 2-D plain-woven C/SiC composite tested at 1200 °C in air. The solid line represents the best-fit.

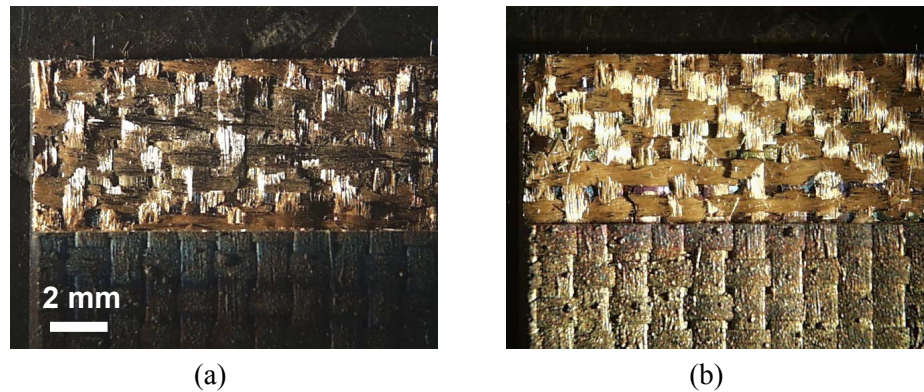


Figure 13.—Fracture surfaces of 2-D plain-woven C/SiC composite specimens subjected to interlaminar shear, tested at 1200 °C in air at: (a) 0.16 MPa/s and (b) 0.00016 MPa/s.

3.1.4. C/SiC Composite

Figure 12 shows the results of interlaminar shear strength testing for the 2-D plain-woven C/SiC composite at 1200 °C in air. Interlaminar shear strength degradation between test rates of 5 and 0.16 MPa/s was negligible. However, below 0.16 MPa/s, shear strength degradation with decreasing test rate was very significant with a resulting degradation of about 90 percent when test rate decreased from 0.16 to 0.00016 MPa/s. The C/SiC composite, in fact, did lose almost its shear-load bearing capability at that lowest test rate with a corresponding value of interlaminar shear strength of only $\tau_f = 2.9 \pm 0.6$ MPa, compared with $\tau_f = 22$ to 24 MPa at higher test rates.

Severe oxidation was observed to have occurred throughout the material body particularly at lower test rates with a change to more yellowish/golden color, as shown in figure 13. Powdered residues were

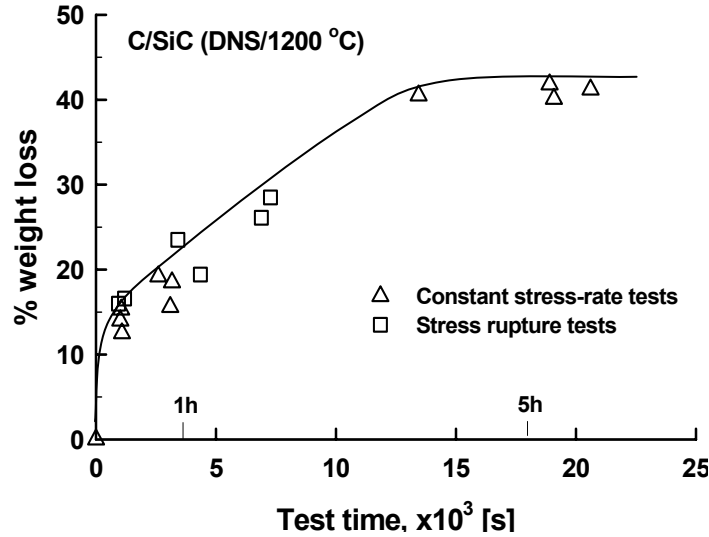


Figure 14.—Weight loss as a function of test time in constant stress-rate and stress rupture testing in interlaminar shear for 2-D plain-woven C/SiC composite tested at 1200 °C in air.

often found from the fracture surfaces of these test specimens, an evidence of oxidation products. Also, weight loss of test specimens after tests was evident: the more weight loss at the lower test rate and vice versa. Figure 14 shows weight loss as a function of test time. The figure also included the weight loss data obtained from stress rupture tests. Regardless of the type of testing, weight loss increased exponentially with test time and reached a plateau around a test time of about 4 hr. The corresponding weight loss at this time was about 40 percent, which is about 80 percent of the original fiber weight fraction. Hence, shear strength degradation of the C/SiC composite was due to oxidation of carbon fibers so that effective number of carbon fibers decreased with time, resulting in a decrease in shear load carrying capability. Evidence of oxidation during testing was also viewed from the nonlinearity of load versus displacement curves. The other composites did not exhibit any measurable weight loss by oxidation and showed little nonlinearity in load versus displacement curves.

4. Discussion

4.1. Model

Strength degradation in tension at elevated temperatures with decreasing test rate occurred in advanced monolithic ceramics including silicon nitrides, silicon carbides, and aluminas (ref. 19). The strength degradation is known as a delayed failure (or fatigue or slow crack growth, SCG) phenomenon, commonly formulated by the empirical power-law relation (ref. 20)

$$v = A(K_I / K_{Ic})^n \quad (3)$$

where v , K_I , and K_{Ic} are crack velocity, stress intensity factor, and fracture toughness under Mode I loading, respectively. A and n are SCG parameters. Based on this power-law relation, the tensile strength (σ_f) can be derived as a function of applied tensile stress rate ($\dot{\sigma}$) with some mathematical manipulations (refs. 14, 15, and 21)

$$\log \sigma_f = \frac{1}{n+1} \log \dot{\sigma} + \log D \quad (4)$$

where D is another SCG parameter dependent on inert strength, n , and crack geometry.

A test method based on equation (4) is called constant stress-rate (or “dynamic fatigue”) testing and has been established as ASTM test methods C 1368 (ref. 14) and C 1465 (ref. 15) to determine SCG parameters of advanced monolithic ceramics at ambient and elevated temperatures. It has been shown that equation (3) was applicable even to CMCs including SiC/CAS (1-D), SiC/MAS-5 (2-D), SiC/SiC (2-D), C/SiC (2-D), and SiC/BSAS (2-D) tested in tension at 1100 to 1200 °C in air, indicating that delayed failure of those composites would be adequately described by the power-law formulation, equation (3). Examples of some of those CMCs exhibiting an invariably significant strength degradation and showing a good data fit to equation (4) are presented in figure 15 (refs. 17 and 18).

It has been also observed that 1-D SiC/BSAS composite exhibited significant strength degradation in shear at 1100 °C in air (ref. 5). A phenomenological model in shear has been proposed and was found to describe well the shear strength dependency of the composite on test rate. The proposed model, similar in expression to the power-law relation of equation (2), takes a following fundamental delayed failure formulation (ref. 5):

$$v_s = \frac{da}{dt} = \alpha_s (K_{II} / K_{IIc})^{n_s} \quad (5)$$

where v_s , a , t , K_{II} , and K_{IIc} are the crack growth rate in shear, crack size, time, Mode II stress intensity factor, and Mode II fracture toughness, respectively. α_s and n_s are delayed failure parameters in shear. In monotonic shear testing, a constant displacement rate or constant force rate is applied to a test specimen until the test specimen fails, so that the shear stress applied to the test specimen is a linear function of test time:

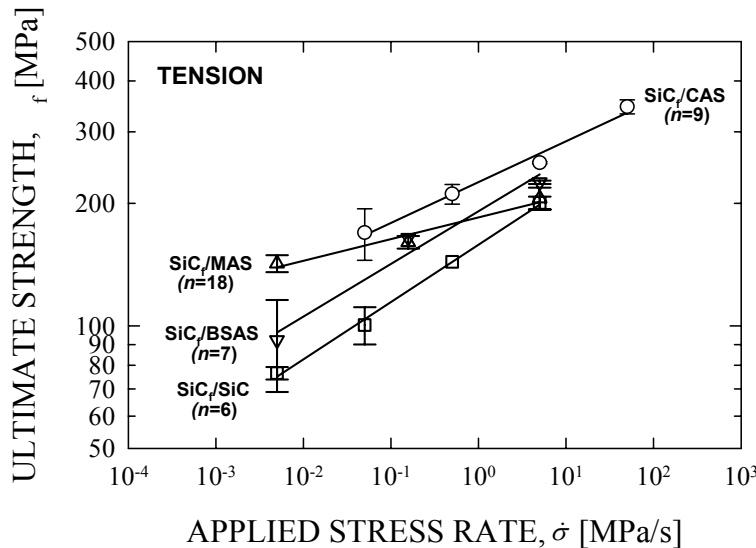


Figure 15.—Examples of ultimate tensile strength as a function of applied stress rate at elevated temperatures in air for various CMCs (refs. 17 and 18) including SiC/MAS (2-D crossplied; 1100 °C), SiC/CAS (1-D; 1100 °C), SiC/SiC (2-D woven; 1200 °C), and SiC/BSAS (2-D crossplied; 1100 °C). The error bars represent ± 1.0 standard deviation.

$$\tau = \int_0^t \dot{\tau}(t) dt = \dot{\tau} t \quad (6)$$

where τ is applied shear stress and $\dot{\tau}$ is applied shear stress rate. The applied shear stress rate $\dot{\tau}$ in displacement control can be determined from the slope ($\Delta P/\Delta t$) of each recorded force-versus-time curve including the portion at or near the point of fracture but excluding the initial nonlinear portion, if any, using a relation $\dot{\tau} = (\Delta P/\Delta t)[1/(WL_n)]$. In case of load control, the applied shear stress rate can be easily obtained from a relation in equation (2). The generalized expression of stress intensity factor (K_{II}) along the crack front of a penny-shaped crack subjected to shear loading either on crack planes or on remote material body (see fig. 16) can take the following form (ref. 21):

$$K_{II} = Y_s \tau a^{1/2} f(\alpha, \varphi) \quad (7)$$

where Y_s is a crack geometry factor also related to a function of $f(\alpha, \varphi)$ with the angles α and φ being defined in figure 16. The K_{II} expression can be significantly simplified when shear stress is aligned with either x_1 or x_2 axis, where the K_{III} component also vanishes, which is the case of the interlaminar shear testing employed in this work. Using equations (5) to (7) and following a similar procedure as used to derive equation (4) in Mode I, one can obtain interlaminar shear strength (τ_f) as a function of applied shear stress rate as follows (ref. 5):

$$\log \tau_f = \frac{1}{n_s + 1} \log \dot{\tau} + \log D_s \quad (8)$$

where D_s is a parameter associated with several constants and other parameters (ref. 5). Equation (8) is analogous to equation (4) for Mode I loading. Delayed failure parameters n_s and D_s in interlaminar shear can be determined from the slope and intercept of a linear regression analysis of the log (*individual interlaminar shear strength with units of MPa*) versus log (*individual applied shear stress rate with units of MPa/s*) data, based on equation (8).

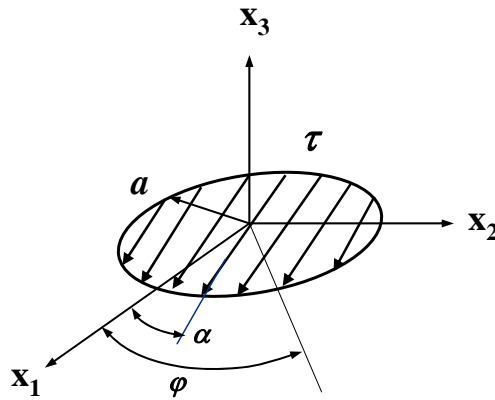


Figure 16.—An assumed penny-shaped crack arbitrarily located at interface between matrix and fibers in ceramic matrix composites, subjected to equal and opposite interlaminar shear stresses τ acting on both surfaces of a crack.

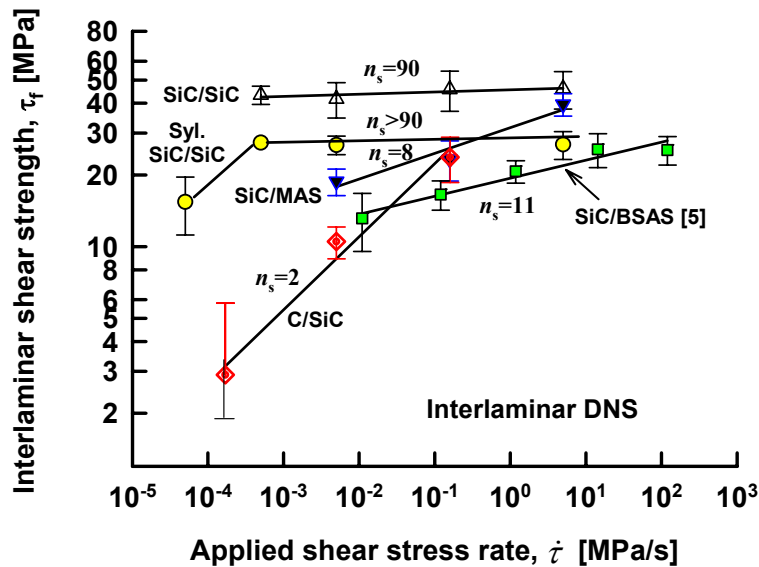


Figure 17.—Summary of interlaminar shear strength as a function of applied shear stress rate for 2-D crossplied SiC/MAS-5 at 1100 °C, 2-D plain-woven SiC/SiC at 1200 °C, 2-D woven Sylramic SiC/SiC at 1316 °C, and 2-D plain-woven C/SiC at 1200 °C in air. The interlaminar shear data on 1-D SiC/BSAS at 1100 °C (ref. 5) is also included. The error bars represent ± 1.0 standard deviation.

A summary of interlaminar shear strength as a function of test rate, based on equation (8), for the CMCs used in this study is shown in figure 17. The average interlaminar shear strength values, instead of individual data points, were used for clarity of illustrations. The level of interlaminar shear strength and the degree of shear strength degradation with respect to test rate are clearly quantified. The figure also includes delayed failure parameters n_s for each composite and the previous result for the SiC/BSAS composite (ref. 5). The reasonable data fit to equation (8) shown in the figure indicates that the fundamental power-law formulation of equation (5) can describe very reasonably the delayed failure behavior under interlaminar shear for the current composite materials. Table 2 is a summary of the parameters n_s and D_s and the coefficients of correlation (r_{coef}) in regression analysis for all the composites.

TABLE 2.—DELAYED FAILURE PARAMETERS OF n_s AND D_s , AND COEFFICIENTS OF CORRELATION (r_{coef}) FOR VARIOUS CMCs DETERMINED IN CONSTANT STRESS-RATE TESTING IN INTERLAMINAR SHEAR AT ELEVATED TEMPERATURES

Composites	Test temperature (°C)	Parameters		
		n_s	D_s	r_{coef}
SiC/MAS-5	1100	8.2 (1.5)	31.8 (2.0)	0.9281
SiC/SiC	1200	88.5	44.8 (2.0)	0.2122
Sylramic SiC/SiC	1316	>90, and 3*	27	-----
C/SiC	1200	2.3 (0.3)	44.7 (7.5)	0.9721
SiC/BSAS (1-D) (ref. 5)	1100	11.2 (2.2)	19.2 (0.9)	0.8442

*The value of n_s for Sylramic SiC/SiC composite was estimated based on the two lowest test rates of 0.00005 and 0.0005 MPa/s (see also fig. 9).

The numbers in parentheses represent ± 1.0 standard deviation.

4.2. Verification of model with stress-rupture data

Constant stress-rate testing in tension has been shown to be a possible alternative to life prediction testing, as verified with stress rupture testing for various CMCs at elevated temperatures of 1100 to 1200 °C (refs. 17 and 18). The underlying reasoning is that the same failure mechanism might have been operative, independent of loading configuration that was either in monotonic ramp (constant stress-rate) loading or in static (stress rupture) loading. In the same way, it would be feasible that life prediction in interlaminar *shear* from one loading configuration to another could be made as far as a single delayed-failure mechanism would be dominant in shear, regardless of loading configuration. A phenomenological life prediction approach was previously proposed based on the data of n_s and D_s using the following relation that accounts for shear loading, which was modified from a relation primarily used for brittle materials in tension (ref. 5):

$$t_f = \left[\frac{D_s^{n_s+1}}{n_s + 1} \right] \tau^{-n_s} f(F) \quad (9)$$

where t_f is time to failure, τ is applied interlaminar shear stress, and $f(F)$ is a functional expression of failure probability and other parameters. Equation (9) determines life as a function of applied interlaminar shear stress, based on n_s and D_s parameters determined from constant shear stress-rate testing for a given probability of failure.

In order to verify the life prediction relation in equation (9), stress rupture testing, aforementioned in the Experimental Procedures section, was conducted for the SiC/MAS-5, Sylramic SiC/SiC, and C/SiC composites. The results of stress rupture testing are presented in figure 18. Significant delayed failure in interlaminar shear occurred in the SiC/MAS-5 and C/SiC composites. Life prediction was made based on equation (9) using the constant stress-rate data n_s and D_s for each composite, and the resulting prediction is presented as a solid line in the corresponding figure with an approximate failure probability of $F = 50$ percent. Despite a limited number of test specimens used, the prediction for the SiC/MAS-5 and C/SiC composites was in good agreement with the stress rupture data, thereby validating equation (9). The prediction for the Sylramic SiC/SiC composite, however, was in poor to reasonable agreement. Note that scatter of time to failure in stress rupture is considerably greater than that of strength in monotonic (constant stress-rate) testing for many brittle materials. Therefore, use of more test specimens is needed for the Sylramic SiC/SiC composite to better verify the proposed model.

Unlike the other CMCs, the C/SiC composite was subjected to significant oxidation of carbon fibers, resulting in material loss. Therefore, strength degradation was increased, attributed to decreasing fiber volume fraction and subsequently increasing porosity. The stress-oxidation model proposed previously (ref. 23) could give a better physical explanation regarding the strength degradation/time dependency phenomenon. However, the phenomenological power-law formulation used in this study still provides a simple, convenient way to quantify the degree of strength degradation with respect to test rate. The oxidation-induced damage would be considered to be equivalent to crack-like flaws growing at matrix-fiber interfaces from a fracture-mechanics point of view. The equivalent crack would propagate under a driving force (K_{II}) based on equation (5) so that the resulting interlaminar shear strength follows equation (8). The fact that there was good agreement between the prediction and the stress rupture data implies that equation (4) would have been operative in delayed failure of the C/SiC composite in interlaminar shear, irrespective of loading configurations. Stress/life behavior and modeling of C/SiC composites in a low partial pressure of oxygen at elevated temperatures in tension can be found elsewhere (refs. 12 and 13).

The results of interlaminar shear strength behavior at elevated temperatures for the four different CMCs showed that constant stress-rate testing could be applicable to determine phenomenological life prediction parameters of the composites even in interlaminar shear. This was evidenced in this work by the results of constant stress-rate testing combined with the results of additional stress rupture testing for

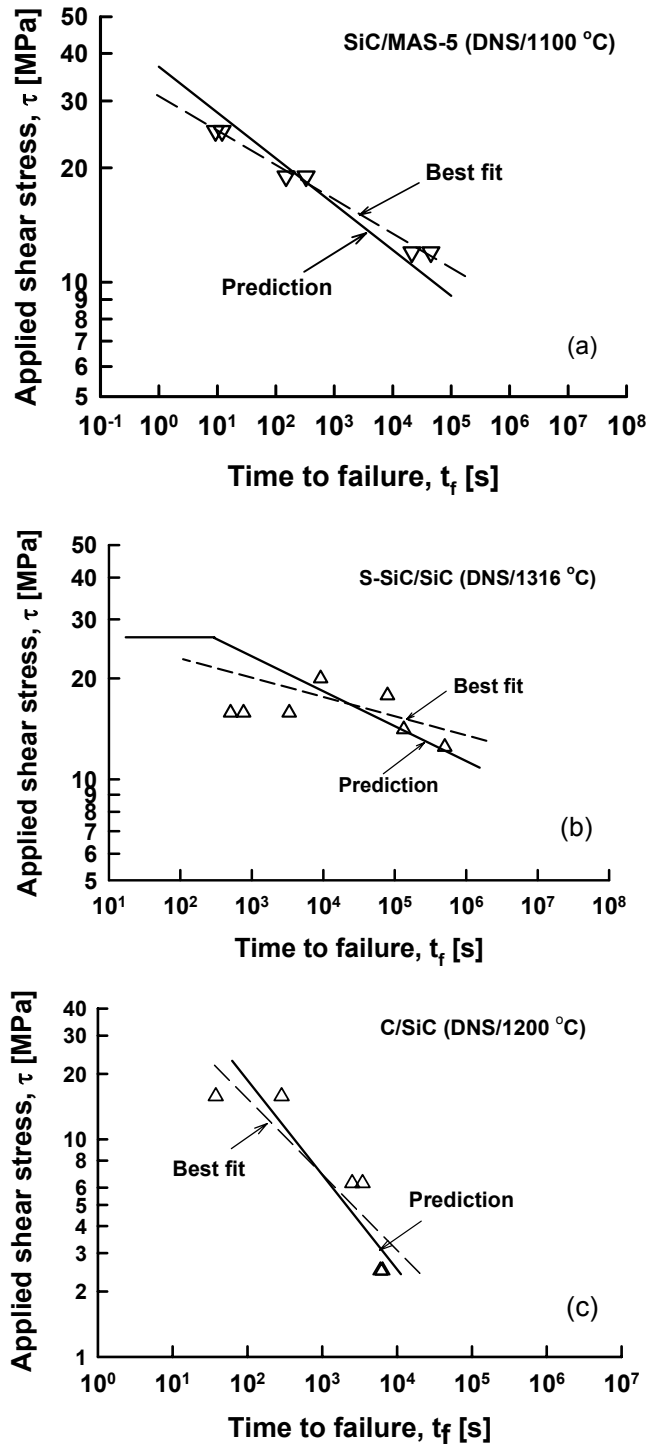


Figure 18.—Results of stress rupture testing in interlaminar shear for: (a) 2-D crossplied SiC/MAS-5 at 1100 °C; (b) 2-D woven Sylramic SiC/SiC at 1316 °C; (c) 2-D plain-woven C/SiC at 1200 °C. Life prediction based on equation (8) is shown as a solid line for each composite. Best-fit line ($\log \tau$ versus $\log t_f$) is also included for each composite.

the three chosen CMCs, indicating that the overall delayed failure mechanism in interlaminar shear could be the one governed by the power-law type of slow crack/damage growth. The merit of constant stress rate testing along with the power-law formulation is enormous in terms of simplicity, test economy (short test times), and less data scatter over other stress rupture or cyclic fatigue testing. Although the experimental results and phenomenological model were presented in this work, a more detailed study of the shear failure mechanism regarding the microscopic influences, which include matrix/fiber interaction, matrix cracking, and environmental effects (refs. 24 to 26), is still needed. It should be kept in mind that the phenomenological model proposed here may incorporate other operative models such as viscous sliding, void nucleation, and coalescence, etc., which can be all covered under a generic term of delayed failure, slow crack growth, fatigue, or damage initiation/accumulation.

Finally, the results of this work also suggest that care must be exercised when characterizing elevated-temperature, interlaminar shear strength of composite materials. This is due to the fact that if a material exhibits a delayed failure phenomenon, elevated-temperature interlaminar shear strength has a relative meaning simply because interlaminar shear strength would depend on which test rate one chooses. Therefore, at least two or three test rates including high and low are recommended to better characterize interlaminar shear strength behavior of a composite material, as suggested previously for the determination of ultimate tensile strength of CMCs at elevated temperatures (refs. 17 and 18).

5. Conclusions

Interlaminar shear strength of four different CMCs including 2-D crossplied SiC/MAS-5, 2-D plain-woven SiC/SiC, 2-D woven Sylramic SiC/SiC, and 2-D plain-woven C/SiC was determined using different test rates at temperatures ranging from 1100 to 1316 °C in air. Interlaminar shear strength degradation in terms of decreasing test rate was significant for SiC/MAS-5 and C/SiC composites and was insignificant for SiC/SiC and Sylramic SiC/SiC composites. The Sylramic SiC/SiC composite, however, exhibited some degree of strength degradation at a very low test rate of 0.00005 MPa/s. A phenomenological, power-law delayed failure model was used to account for interlaminar shear strength degradation and showed good agreement with SiC/MAS-5 and C/SiC composites but in poor to reasonable agreement with Sylramic SiC/SiC composite, as compared with the additional stress rupture results. Constant-shear stress-rate testing could be a possible means of life prediction test methodology for composites in interlaminar shear in case that short lifetimes of components are anticipated.

References

1. P. Brondsted, F.E. Heredia, and A.G. Evans, "In-Plane Shear Properties of 2-D Ceramic Composites," *J. Am. Ceram. Soc.*, 77[10] 2569–2574 (1994).
2. E. Lara-Curzio and M.K. Ferber, "Shear Strength of Continuous Fiber Ceramic Composites," ASTM STP 1309, p. 31, American Society for Testing and Material, West Conshohocken, PA (1997).
3. N.J.J. Fang and T.W. Chou, "Characterization of Interlaminar Shear Strength of Ceramic Matrix Composites," *J. Am. Ceram. Soc.*, 76[10] 2539–2548 (1993).
4. Ö. Ünal and N.P. Bansal, "In-Plane and Interlaminar Shear Strength of a Unidirectional Hi-Nicalon Fiber-Reinforced Celsian Matrix Composite," *Ceramics International*, 28 527–540 (2002).
5. S.R. Choi, N.P. Bansal, A.M. Calomino, and M.J. Verilli, "Shear Strength Behaviors of Ceramic Matrix Composites at Elevated Temperatures," *Advanced in Ceramic Matrix Composites*, Edited by J.P. Singh, N.P. Bansal, and W.M. Kriven, Ceramic Transactions Vol. 165, 131–145 (2005).
6. S.R. Choi and N.P. Bansal, "Shear Strength as a Function of Test Rate for SiC_f/BSAS Ceramic Matrix Composite at Elevated Temperature," *J. Am. Ceram. Soc.*, 87[10] 1912–1918 (2004).
7. D.W. Worthem, "Thermomechanical Fatigue Behavior of Three CFCCs," NASA CR-195441, National Aeronautics and Space Administration, Glenn Research Center, Cleveland, OH (1995).

8. D. Brewer, "HSR/EPM Combustor Materials Development Program," *Mat. Sci. Eng.*, A261 284–291 (1999).
9. A. Calomino, "Mechanical Behavior and Characterization 1316 °C In-situ BN Coated MI/SiC/SiC," *Technology Forum October 2002*, Ultra-Efficient Engine Technology Program, NASA Glenn Research Center, Cleveland, Ohio (2002).
10. A. Calomino and M. Verrilli, "Ceramic Matrix Composite Vane Subelement Fabrication," *Proceedings of ASME Turbo Expo 2004*, June 14–17, Vienna, Austria, ASME Paper No. GT2004–53974.
11. M. Verrilli, A. Calomino, R.C. Robinson, and D.J. Thomas, "Ceramic Matrix Composites Vane Subelement Testing in a Gas Turbine Environment," *ibid.*, ASME Paper No. GT2004–53970.
12. M.J. Verrilli, A. Calomino, and D.J. Thomas, "Stress/Life Behavior of a C/SiC Composite in a Low Partial Pressure of Oxygen Environment: I- Static Strength and Stress Rupture Database," *Ceram. Eng. Sci. Proc.*, 23[3] 435–442 (2002).
13. A. Calomino, M.J. Verrilli, and D.J. Thomas, "Stress/Life Behavior of a C/SiC Composite in a Low Partial Pressure of Oxygen Environment: II- Stress Rupture Life and Residual Strength Relationship," *ibid.*, 23[3] 443–451 (2002).
14. ASTM C 1368, "Standard Test Method for Determination of Slow Crack Growth Parameters of Advanced Ceramics by Constant Stress-Rate Flexural Testing at Ambient Temperature," *Annual Book of ASTM Standards*, Vol. 15.01, American Society for Testing and Materials, West Conshohocken, PA (2003).
15. ASTM C 1465, "Standard Test Method for Determination of Slow Crack Growth Parameters of Advanced Ceramics by Constant Stress-Rate Flexural Testing at Elevated Temperatures," *Annual Book of ASTM Standards*, Vol. 15.01, American Society for Testing and Materials, West Conshohocken, PA (2003).
16. ASTM C 1425, "Test Method for Interlaminar Shear Strength of 1-D and 2-D Continuous Fiber-reinforced Advanced Ceramics at Elevated Temperatures," *Annual Book of ASTM Standards*, Vol. 15.01, American Society for Testing and Materials, West Conshohocken, PA (2002).
17. S.R. Choi and J.P. Gyekenyesi, "Load-Rate Dependency of Ultimate Tensile Strength in Ceramic Matrix Composites at Elevated Temperatures," *Int. J. Fatigue*, 27 503–510 (2005).
18. S.R. Choi, N.P. Bansal, and M.J. Verrilli, "Delayed Failure of Ceramic Matrix Composites in Tension at Elevated Temperatures," *J. Euro. Ceram. Soc.*, 25 1629–1636 (2005).
19. S.R. Choi and J.P. Gyekenyesi, "'Ultra'-Fast Fracture Strength of Advanced Structural Ceramics at Elevated Temperatures: An Approach to High-Temperature 'Inert' Strength," pp. 27–46 in *Fracture Mechanics of Ceramics*, Vol. 13, Edited by R.C. Bradt, D. Munz, M. Sakai, V. Ya. Shevchenko, and K.W. White, Kluwer Academic/Plenum Publishers, New York (2002).
20. S.M. Wiederhorn, "Subcritical Crack Growth in Ceramics," pp. 613–646 in *Fracture Mechanics of Ceramics*, Vol. 2, Edited by R.C. Bradt, D.P.H. Hasselman, and F.F. Lange, Plenum Press, New York (1974).
21. A.G. Evans, "Slow Crack Growth in Brittle Materials under Dynamic Loading Condition," *Int. J. Fracture*, 10 251–259 (1974).
22. H. Tada, P.C. Paris, and G.R. Irwin, *The Stress Analysis of Cracks Handbook*, Part IV. The American Society of Mechanical Engineers, New York, 2000.
23. M.C. Halbig, "Modeling the Oxidation of Carbon Fibers in a C/SiC Composite under Stressed Oxidation," *Ceram. Eng. Sci. Proc.*, 23[3] 427–434 (2002).
24. C.A. Lewinsohn, C.H. Henager, and R.H. Jones, "Environmentally Induced Time-Dependent Failure Mechanism in CFCCs at Elevated Temperatures," *Ceram. Eng. Sic. Proc.*, 19[4] 11–18 (1998).
25. C.H. Henager and R.H. Jones, "Subcritical Crack Growth in CVI Silicon Carbide Reinforced with Nicalon Fibers: Experiment and Model," *J. Am. Ceram. Soc.*, 77[9] 2381–94 (1994).
26. S.M. Spearing, F.W. Zok, and A.G. Evans, "Stress Corrosion Cracking in a Unidirectional Ceramic-Matrix Composite," *J. Am. Ceram. Soc.*, 77[2] 562–70 (1994).

REPORT DOCUMENTATION PAGE			Form Approved OMB No. 0704-0188	
Public reporting burden for this collection of information is estimated to average 1 hour per response, including the time for reviewing instructions, searching existing data sources, gathering and maintaining the data needed, and completing and reviewing the collection of information. Send comments regarding this burden estimate or any other aspect of this collection of information, including suggestions for reducing this burden, to Washington Headquarters Services, Directorate for Information Operations and Reports, 1215 Jefferson Davis Highway, Suite 1204, Arlington, VA 22202-4302, and to the Office of Management and Budget, Paperwork Reduction Project (0704-0188), Washington, DC 20503.				
1. AGENCY USE ONLY (Leave blank)		2. REPORT DATE January 2006		3. REPORT TYPE AND DATES COVERED Technical Memorandum
4. TITLE AND SUBTITLE Life Limiting Behavior in Interlaminar Shear of Continuous Fiber-Reinforced Ceramic Matrix Composites at Elevated Temperatures			5. FUNDING NUMBERS WBS-22-714-30-19	
6. AUTHOR(S) Sung R. Choi, Anthony M. Calomino, Narottam P. Bansal, and Michael J. Verrilli				
7. PERFORMING ORGANIZATION NAME(S) AND ADDRESS(ES) National Aeronautics and Space Administration John H. Glenn Research Center at Lewis Field Cleveland, Ohio 44135-3191			8. PERFORMING ORGANIZATION REPORT NUMBER E-15425	
9. SPONSORING/MONITORING AGENCY NAME(S) AND ADDRESS(ES) National Aeronautics and Space Administration Washington, DC 20546-0001			10. SPONSORING/MONITORING AGENCY REPORT NUMBER NASA TM-2006-214088	
11. SUPPLEMENTARY NOTES Sung R. Choi, University of Toledo, 2801 W. Bancroft St., Toledo, Ohio 43606; and Anthony M. Calomino, Narottam P. Bansal, and Michael J. Verrilli (now with G.E. Aircraft Engines), NASA Glenn Research Center. Responsible person, Sung R. Choi, organization code RXL, 216-433-8366.				
12a. DISTRIBUTION/AVAILABILITY STATEMENT Unclassified - Unlimited Subject Category: 07 Available electronically at http://gltrs.grc.nasa.gov This publication is available from the NASA Center for AeroSpace Information, 301-621-0390.			12b. DISTRIBUTION CODE	
13. ABSTRACT (Maximum 200 words) Interlaminar shear strength of four different fiber-reinforced ceramic matrix composites was determined with double-notch shear test specimens as a function of test rate at elevated temperatures ranging from 1100 to 1316 °C in air. Life limiting behavior, represented as interlaminar shear strength degradation with decreasing test rate, was significant for 2-D crossplied SiC/MAS-5 and 2-D plain-woven C/SiC composites, but insignificant for 2-D plain-woven SiC/SiC and 2-D woven Sylramic (Dow Corning, Midland, Michigan) SiC/SiC composites. A phenomenological, power-law delayed failure model was proposed to account for and to quantify the rate dependency of interlaminar shear strength of the composites. Additional stress rupture testing in interlaminar shear was conducted at elevated temperatures to validate the proposed model. The model was in good agreement with SiC/MAS-5 and C/SiC composites, but in poor to reasonable agreement with Sylramic SiC/SiC. Constant shear stress-rate testing was proposed as a possible means of life prediction testing methodology for ceramic matrix composites subjected to interlaminar shear at elevated temperatures when short lifetimes are expected.				
14. SUBJECT TERMS Continuous fiber-reinforced ceramic matrix composites; Mechanical testing; Double notch shear testing; Constant stress-rate testing in shear; Stress rupture in shear; Life prediction; Life prediction methodology			15. NUMBER OF PAGES 25	
			16. PRICE CODE	
17. SECURITY CLASSIFICATION OF REPORT Unclassified	18. SECURITY CLASSIFICATION OF THIS PAGE Unclassified	19. SECURITY CLASSIFICATION OF ABSTRACT Unclassified	20. LIMITATION OF ABSTRACT	

